Photoemission Investigation of the Electronic Structure of Chromium*

GERALD J. LAPEYRE AND KENNETH A. KRESS†
Department of Physics, Montana State University, Bozeman, Montana
(Received 21 August 1967)

Photoemission measurements of the quantum yield and energy distributions are obtained from evaporated films of Cr in the spectral range from 4.68 (threshold) to 11.8 eV. Data are obtained at room temperature, at liquid-air temperature, and above the Néel temperature. No evidence is found that the conservation of the Bloch-state wave vector is important in the optical excitations. The temperature dependence shows that the excitations are not phonon-assisted. The nondirect transition model is used to obtain the optical density of filled states, N_v, and of empty states, N_c. The matrix elements for the excitation are approximately constant. N_v has a peak at $E-E_F=-5.5\pm0.3$ eV that corresponds to the anomalous peak observed in Fe, Co, and Ni, which is not predicted by band calculations. E_F is the Fermi energy. N_v has peaks at $E-E_F$ equal to -1.1 ± 0.2 and -2.2 ± 0.2 eV and a shoulder at 0.2 eV. The properties of N_v show that the rigid-band model is invalid for obtaining the Cr density of states from that for Fe. N_v near E_F correlates with specific-heat results. No structure is observed in N_c above the vacuum energy and the empty d bands are found to be approximately 1.5 eV wide by analyzing the quantum yield. The photodiode is used to obtain a semi-quantitative measure of the reflectance, which contains structure that is consistent with the anomalous peak in N_v. The quantum yield and reflectance show a feature at 9.4 eV that is suggestive of a surface or impurity plasmon and show no significant effects on the energy distributions of the emitted electrons. Studies above and below the Néel temperature show that electronic-structure changes due to magnetic ordering are too small to be observed, i.e., no greater than 0.3 eV.

I. INTRODUCTION

THE electronic structure of the transition metals has been the object of many investigations. A principal motivation for the investigations is the magnetic phenomena exhibited by the metals. Photoemission measurement provides a technique for investigating electronic structure over wide energy ranges. Spicer and collaborators have used the photoemission technique to study the first series transition metals, Cu,[1] Ni,[2] Co,[3] and Fe.[4] The present work has used the photoemission technique to study the electronic structure of chromium.

Photoemission data have been obtained from evaporated films of Cr in the spectral range from the threshold at 4.68 eV to the optical cutoff of LiF at 11.8 eV. Data are obtained for liquid-air temperature, room temperature, and above the Néel temperature. The experimental design of the photodiode used permitted one to obtain indirect reflectance data on Cr. The results show that the optical transitions are nondirect in Cr. The nondirect transition model used to analyze Cu, Ni, Co, and Fe is used to analyze the present data, and the optical density of states is obtained. The Cr density of states is remarkably similar to those obtained for the other metals studied and exhibits the anomalous peak at low energies.[3] The temperature dependence shows the optical transitions are not phonon-assisted and that the electronic-structure changes, due to magnetic ordering, are small (<0.3 eV). A feature at 9.4 eV is observed which is suggestive of an impurity or surface plasma mode.

Section II describes the experimental setup and the technique which use the photodiode to obtain a semi-quantitative measurement of the reflectivity. The data are presented in Sec. III. The nondirect model is used to analyze the data in Sec. IV, and the results are discussed in Sec. V.

II. EXPERIMENTAL PROCEDURE

The photodiode geometry which has been used by other investigators[5,6] consists of a cylindrical collector and a flat polished cathode. Each element is placed on the end of a ceramic, insulated liquid-nitrogen Dewar. The cathode, consisting of a $\frac{3}{4}$-in. diam copper rod, bolts into a copper ring which serves as the plug for one Dewar. The cathode is rolled from a $\frac{1}{16}$-in. copper sheet and is bolted to the second Dewar.

The diode-Dewar system was placed in a 4-in.-diam all-metal ultra-high-vacuum system which was continuously pumped with a 15 liter/sec ion pump. Consistent pressures better than 1×10^{-9} Torr were ob-

* Research sponsored by the Air Force Office of Scientific Research, Office of Aerospace Research, U.S. Air Force, under AFOSR Contract/Grant No. AF-AFOSR-838-65.
† Supported in part by a National Aeronautics and Space Administration Traineeship.
[1] C. N. Berglund and W. E. Spicer, Phys. Rev. **136**, A1030 (1964); **136**, A1044 (1964); W. E. Spicer, in *Optical Properties and Electronic Structure of Metals and Alloys*, edited by F. Abèles (North-Holland Publishing Co., Amsterdam, 1966), p. 296; C. N. Berglund, in *Optical Properties and Electronic Structure of Metals and Alloys*, edited by F. Abèles (North-Holland Publishing Co., Amsterdam, 1966), p. 285.
[2] A. J. Blodgett, Jr. and W. E. Spicer, Phys. Rev. **146**, 390 (1966); Phys. Rev. Letters **15**, 20 (1965).
[3] A. Y.-C. Yu and W. E. Spicer, Phys. Rev. Letters **23**, 1171 (1966).
[4] A. J. Blodgett and W. E. Spicer, Phys. Rev. **158**, 514 (1967); W. E. Spicer, J. Appl. Phys. **37**, 947 (1966).
[5] W. E. Spicer and C. N. Berglund, Rev. Sci. Instr. **35**, 1665 (1964).
[6] N. B. Kindig and W. E. Spicer, Rev. Sci. Instr. **36**, 759 (1965).

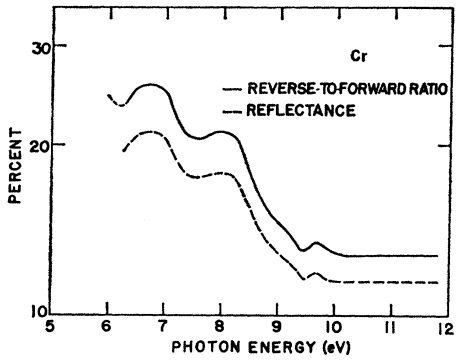

FIG. 1. Spectral dependence of the reverse-to-forward ratio of the diode current at an incidence angle of 10° and the reflectance obtained from the ratio for chromium.

tained. The chamber contained an LiF window for transmission of the exciting radiation.[6] The LiF was sealed with AgCl.

The chromium was evaporated onto the cathode and the inside of the collector can. Electrolytically deposited Cr was used,[7] and it was evaporated by resistance heating of a tungsten basket containing the source material. During final deposition of the films, the pressure was in the upper 10^{-9} Torr range.

The diode design permits the determination of the energy distribution of the emitted electrons (EDC) by differentiation of the retarding potential versus current characteristics.[5] The differentiation was done electronically by applying an ac voltage to the retarding potential. The ac level was 40 mV rms and the optical band pass was 8 Å wide.

The photodiode geometry was also used to obtain information about the reflectance of the Cr films. The procedure was to turn the diode 10° with respect to the incident optical beam, so that the reflection from the cathode struck the collector. The geometry of the diode was such that the reflection from the collector also struck the collector. For this geometry, the ratio of the reverse to the forward current (RFR) is related to the reflectance of the samples since all surfaces are covered with a Cr film. Neglecting the third reflection and assuming the reflectance (R) and the quantum yield to be angularly independent, the following relation is obtained:

$$\mathrm{RFR}=r\approx R+R^2. \qquad (1)$$

The assumptions are reasonable because the reflectance is less than 30%, the average angle of the first reflection is 10°, and the average angle of the second reflection is 25°. The angular dependence observed for Cr at a photon energy of 2.1 eV is small for these angles.[8] The ratio of the reverse to forward current is considered to be a semiquantitative measure of the reflectance.

III. DATA

A. Reverse-to-Forward Ratio

The reverse-to-forward ratio (RFR) obtained with the incident optical beam at an angle of 10° with respect to the diode is shown in Fig. 1. The reflectance is calculated by using Eq. (1). Since the RFR is a small number, the approximations used to obtain Eq. (1) are reasonable and a semiquantitative value of the spectral reflectance is obtained. The results are shown in Fig. 1.

B. Quantum Yield

The spectral dependence of the quantum yield was obtained with a sodium salycilate coated commercial phototube. Data were taken with a fresh sodium salycilate film and with a film left in vacuum for several months. The spectral dependence of the quantum yield obtained with the aged film increases faster above 9 eV than the result obtained with a fresh film. The results using fresh sodium salycilate are used in this study. Vacuum-aging studies have shown that the spectral response decreases with age at the higher photon energy.[9]

The magnitude of the yield was obtained by comparing it with that from a calibrated phototube in the spectral range between 5 and 6 eV. This procedure is difficult, and the calibration could be in error by as much as 20%.

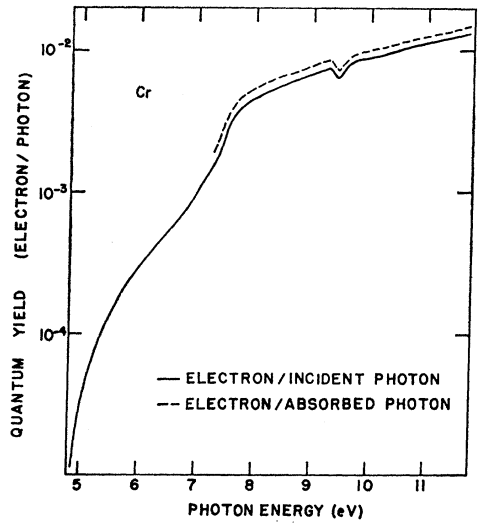

FIG. 2. The spectral dependence of the quantum yield of chromium. The correction for the reflectance is obtained from the reverse-to-forward ratio.

[7] The Cr was obtained from Abner Brenner, National Bureau of Standards, Washington, D.C.

[8] F. Abèles, J. Opt. Soc. Am. **47**, 473 (1957).

[9] W. E. Spicer (private communication).

The quantum yield per incident photon is shown in Fig. 2. The figure also shows the yield per absorbed photon obtained with the RFR data.

The photoelectric threshold of 4.68 eV is obtained from a linear fit to the square root of the yield as a function of photon energy. This functional dependence for the threshold region is predicted by Fowler's theory.[1,10] Figure 3 shows the results for liquid-air temperature. The data at room temperature give a slightly lower value (about 0.06 eV less).

The structure observed at 9.4 eV is weak. It is difficult to attribute it to anomalies in spectral response of sodium salycilate or the spectral transmission of the LiF window on the experimental chamber, since it is also observed in the RFR data. The depth of the minimum showed some dependence on the quality of

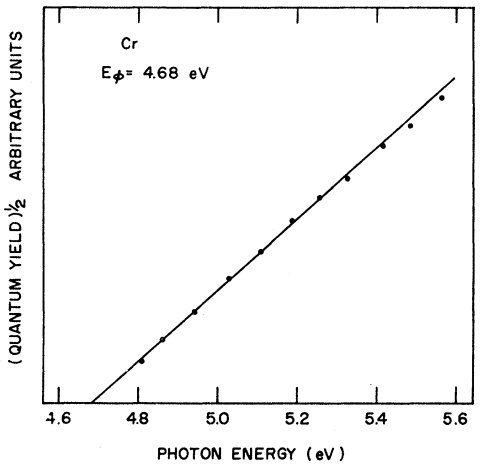

FIG. 3. Determination of the work function of chromium at liquid-air temperature.

the sample. On a well-prepared film at high vacuum, the depth varied from about 10 to 15% and increased slightly as the film aged from 2 to 90 days. A poorly prepared film studied when it was 6 months old showed a 40% dip.[11] The poorly prepared film was formed very slowly in the 10^{-8}-Torr region. The details of this phenomenon have not been pursued in this study.

C. Energy Distribution of Photoemitted Electrons

The energy distribution curves (EDC's) for the spectral range near the threshold are shown in Fig. 4. For reasons discussed in Sec. IV, the curves are plotted as a function of $E-h\nu$. The EDC's in Fig. 4 have not been normalized to the yield. A representative set of EDC's for $7.3 \leq h\nu \leq 11.8$ are shown in Figs. 5 and 6. The noise level for the EDC at 11.8 eV is significant,

[10] R. H. Fowler, Phys. Rev. **38**, 45 (1931).

[11] EDC's obtained on this sample showed strong attenuation of the high kinetic-energy electrons and a very large low kinetic-energy peak for $h\nu > 9.7$ eV.

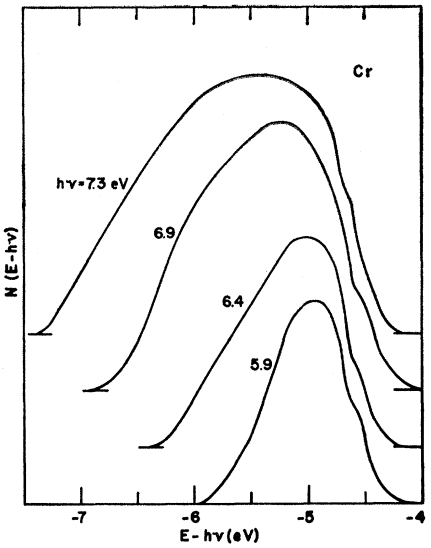

FIG. 4. Energy distributions of photoemitted electrons from chromium at liquid-air temperature plotted versus $E-h\nu$ for $h\nu \leq 7.3$ eV. The curves are not normalized to the quantum yield.

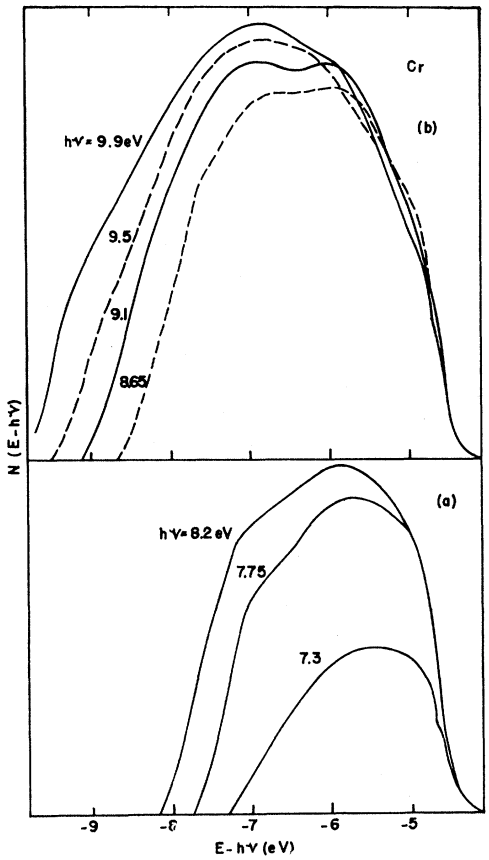

FIG. 5. Energy distributions of photoemitted electrons from chromium at liquid-air temperature plotted versus $E-h\nu$ for $7.3 \leq h\nu \leq 9.9$ eV. The curves are normalized to the quantum yield.

but the general shape of the curve is reliable. The latter curves have been normalized to the yield as corrected with the RFR data. Since the reflectance correction to the yield is small, the qualitative nature of the reflectance data is not important. The shoulder at maximum kinetic energy in the EDC's for $h\nu \leq 7.3$ eV is also present at the higher photon energies, but it is too small to be discerned on the scale used. The data shown in Figs. 4–6 were taken at liquid-air temperature. Details of the temperature dependence are discussed later.

The EDC's showed a small age effect when a film 24 h old was compared with a film 2 h old. The number of high kinetic-energy electrons was attenuated slightly, less than 2%. This attenuation is attributed to scattering by absorbed gas on the surface. The data presented were taken on a film before it was 3 days old. Over a period of a few days no additional changes were noted.

D. Temperature Dependence

A set of photoemission data was taken at liquid-air temperature and above the Néel temperature in addition to a set of room-temperature data. Both elements of the diode were at the same temperature. The high-temperature data were taken by heating the diode elements about 30°C above the Néel temperature (40°C), and then the heaters were disconnected so that they did not interfere with the analysis instrumentation. The procedure netted about 2 h working time for the photoelectric studies.

The temperature dependence of the yield was studied by two different procedures. First, the spectral response at a given temperature was measured as previously described. Second, three photon energies were selected (7.8, 10.2, and 11.5 eV), and the yield was measured as a function of temperature. During the latter procedure, the only instrumental change made was the cooling and heating of the sample. The light intensity was monitored so that lamp drifts could be corrected.

The shape of the yield curve determined by the first procedure at all three temperatures is within the limits of accuracy of the experiment.

Measurements of the yield at a spectral point as a function of temperature showed very weak temperature dependence. The magnitude of the changes observed are not significantly larger than the expected error. For example, one set of data at $h\nu = 10.2$ eV showed that the yield increased 4% on heating above 50°C, decreased 2% on cooling to room temperature, and increased 3% on cooling to liquid-air temperature. This example is typical of all the data taken at the three photon energies.

The changes on cooling to liquid-air temperature were reasonably consistent. However, the changes resulting from heating above the Néel point were erratic and they always showed hysteresis. Since the accuracy of the procedure is not better than a few percent, no significance should be attributed to the magnitude of the changes. The observation that the yield increases slightly on cooling from 300 to 85°K is considered to be real.

A set of EDC's were taken at 300, 85, and >323°K. The differences observed are very small and are not considered to be larger than the uncertainties in the measurements. A representative sample of the data is shown in Fig. 7. Differences are more difficult to measure above $h\nu > 11.0$ eV since the light flux is much weaker.

IV. ANALYSIS OF THE DATA

The dominant feature of the set of EDC's shown in Figs. 5 and 6 is the fixed position of the three shoulders at $E-h\nu$ equal to -4.9, -5.8, and -6.9 eV and the superposition of the curves for the spectral range up to 11.8 eV. As the analysis will demonstrate, this property of the data means first, that the dominant selection rule for the optical transitions is energy conservation, and second, that the structure observed in the EDC's is due to structure in the occupied states N_v. The first property shows that the data fit the nondirect optical-transition model where the conservation of **k**, the Bloch-state wave vector, is not an important optical-selection rule.[12] The model has been used to interpret the photoemission data from Fe,[4] Co,[3] Ni,[2] and the d bands of Cu.[1]

In the nondirect transition model, the energy distribution of the photoemitted electrons is given by

$$N(E) = CT(E)N_c(E)N_v(E-h\nu) \qquad (2)$$

if electron scattering is neglected.[13] T is the escape function; N_c and N_v are the optical densities of empty states and occupied states, respectively. C is a constant which contains the matrix element between the initial and final states which to a first approximation is assumed constant for the present analysis. The analysis will show that this is a reasonable approximation as it is for the other transition metals studied.

Inspection of Eq. (2) shows that structure in the initial states N_v will appear at a fixed position in a set of EDC's when the curves are plotted as a function of $E-h\nu$. When the EDC's are plotted as a function of E, the position of a structure point due to the initial states will increase at the same rate as the photon energy increases. The reverse of this phenomenon occurs for structure in the final states.

With Eq. (2), a set of EDC's can be analyzed to obtain the optical density of states below the Fermi

[12] If **k** is not directly conserved, the terminology "**k** not important (KNIMP)" is used in the cited literature. When **k** is not important and the transitions are not phonon-assisted, they are termed "nondirect." The excitations observed here are not phonon-assisted.

[13] For a detailed discussion of the model and scattering effects see the cited literature, particularly Refs. 1 and 2.

energy and the product of the density of states multiplied by the escape function above the vacuum energy.

A. Optical Density of States for $-4 \leq E-F_F \leq 0$ and $4.68 \leq E-E_F \leq 11.8$ eV

Equation (2) was first used to obtain the density of states between E_F and $E-E_F=-4$. The procedure used was essentially one of trial and error. The procedure was initiated by normalizing the magnitudes of succeeding EDC's in their respective kinetic-energy (KE) regions around 2.5 eV on an $E-h\nu$ plot. Then the envelope was used to obtain a density-of-states function between E_F and $E-E_F=-4$ eV. In the region around KE$=2.5$ eV, the EDC's are least affected by the escape function and their observed attenuation at high KE. The latter feature will be discussed later. The resultant density-of-states function and TN_v are shown in Figs. 8 and 9, respectively. The latter result

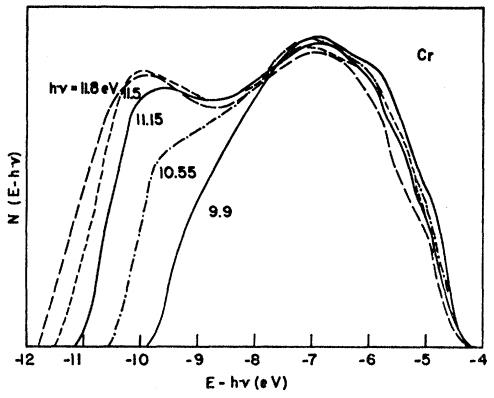

FIG. 6. Energy distributions of photoemitted electrons from chromium at liquid-air temperature plotted versus $E-h\nu$ for $9.9 \leq h\nu \leq 11.8$ eV. The curves are normalized to the quantum yield.

shows that the density of states above the vacuum level is essentially constant since the shape of the curve near the vacuum level results from the escape cone.[1] To demonstrate the self-consistency of the above procedure, a set of EDC's was computed for $8.2 \leq h\nu \leq 10.2$ eV. The comparison of the computed results with the data is shown in Fig. 10. Considering the simplicity of the model, the results are good. The results show that **k** conservation is not an important selection rule, and that the energy dependence of the matrix elements are constant to a first approximation.

The attenuation of the EDC's near maximum KE is a result of the loss of emitted electrons by electron-electron scattering (see Figs. 5, 6, and 10). This scattering effect increases as the energy increases. These same scattering features have been observed in the photoemission studies on other metals and are discussed in detail in Refs. 1 and 2. Lifetime broadening also contributes to this attenuation.[1]

The small shoulder observed at the maximum KE

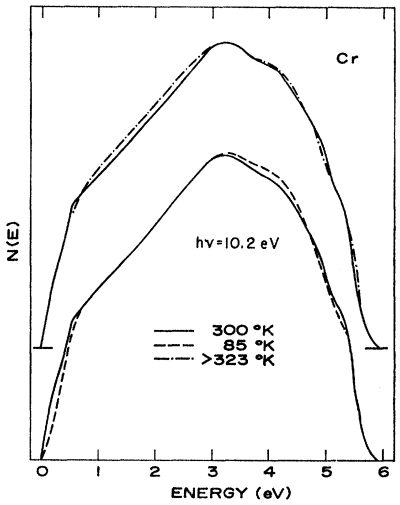

FIG. 7. Energy distributions of photoemitted electrons from chromium at liquid-air temperature, room temperature, and above the Néel temperature for $h\nu=10.2$ eV.

in the EDC's is the density of states just below the Fermi energy. See Fig. 4. The shoulder is too small to be displayed on the scale used for Figs. 5 and 6. The shoulder is observed at about $E-h\nu=-4.6$ eV, in the EDC's which is slightly higher than the threshold energy. This is to be expected because the optical band pass and ac modulating signal used to obtain the EDC's shifts a steeply decreasing shoulder to higher energy by approximately this amount.

B. Density of States for $E-E_F<-4$ eV

The analysis of the low KE contribution to the EDC's for $h\nu>10.2$ eV is difficult because of the spectral limit of the LiF window used in the experiment. As a result of the spectral limit and the effects of the escape function, the dependence of the structure on the photon energy cannot be examined. Several features of the experiment suggest that the low energy contribution is due to deep valence band states and not the emission of electrons which have been electron-electron scattered. The reasons are indirect and are presented below.

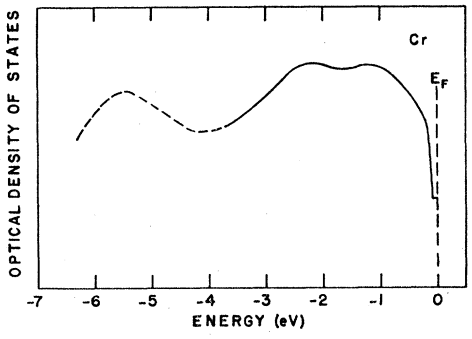

FIG. 8. Filled band optical density of states for chromium.

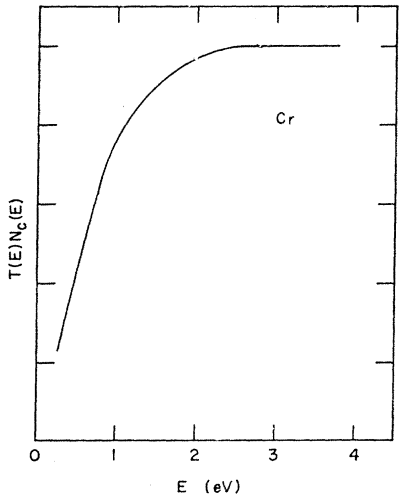

FIG. 9. The product $T(E)Nc(E)$ for chromium.

First, a density of states at low energy is obtained by dividing the EDC's under consideration by the escape function which was obtained in the above analysis. The resulting functions are normalized at $E-h\nu=-8.5$ eV and plotted as functions of $E-h\nu$. A peak about -10.2 eV is obtained which shows reasonable superposition for each computed curve. Two of the computed curves are shown in Fig. 11. This computation assumes that **k** conservation is not an important selection rule. Because of the experimental limit on the spectral range, this assumption cannot be directly tested with the data. One would not expect the character of the transitions under consideration to be different from the transitions for $h\nu<10.2$ eV, which are shown above to be nondirect. If the high-energy transitions were direct, the structure being discussed would require structure above the vacuum level. Structure above the vacuum level is not observed (see the preceding discussion). Use of the assumption of nondirect transitions for the states under consideration gives reasonable results for the shape of the spectral dependence of the quantum yield (see the Appendix). Analogous deep-lying states are observed in Ni [2] and Fe,[4] where reasonable evidence exists that the transitions are nondirect (see Sec. V). The assumption that these high-energy transitions are nondirect appears to be reasonable.

Second, the character of emitted electrons which have been scattered inelastically is different from the emission observed in these data. The number of scattered electrons should monotonically increase as their KE decreases. Thus emission of scattered electrons should produce a maximum near zero KE in the energy distribution. The function N/T would monotonically increase. In Cu and Ag, scattered electrons are observed in the EDC's and form a peak at KE$=0.5$ eV, independent of the value of $h\nu$. The magnitude of the scattered peak, on the other hand, increases with $h\nu$. Neither of these characteristics is observed in the present data.

Third, for the data in question to be entirely due to scattered electrons, the number of electrons lost at high KE in the EDC's would have to be much larger than the number of scattered electrons emitted since most would have insufficient energy to escape. To demonstrate this conservation effect, the EDC to be expected in the absence of scattering is also shown in Fig. 11, the density of states. Observation of Fig. 11 shows that the number of electrons scattered out of the EDC is considerably smaller than the number of observed electrons at low KE.

The energy-distribution curves for $h\nu>10.2$ eV (in Fig. 6), which are normalized to the yield, show the low KE energy peak is not emitted at the expense of the high KE peak, as the above interpretation requires.

Fourth, structure in the neighborhood of -5.5 eV in the density of states correlates with the structure observed in the RFR data. The energetics of the correlation is described below. The present optical data are insufficient to do a detailed analysis. RFR data, and thus the reflectance, have a peak at about 6.8 eV and a

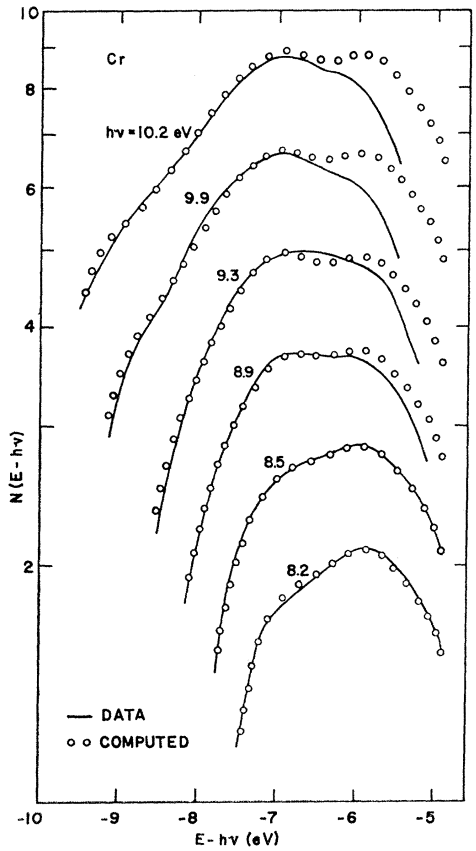

FIG. 10. Comparison of the energy-distribution curves computed from the optical density of states to the data curves. The logarithm of the amplitudes are plotted versus $E-h\nu$.

pronounced shoulder about 8.0 eV. These features mean that the optical conductivity has structure in this spectral region. For nondirect transitions, the optical conductivity for constant matrix elements is given by

$$\omega\sigma(\omega) = B\int_{E_F}^{E_F-h\nu} N_c(E)N_v(E-h\nu)\,dE. \qquad (3)$$

The terms are the same as those used in Eq. (2). Examination of Eq. (3) shows that optical structure in the neighborhood of 7 eV results from coupling between the low-energy states in the filled band and the empty d states between the Fermi energy and the vacuum energy. The empty d bands are estimated to extend approximately 1.5 eV above the Fermi energy. See the Appendix for a discussion of the states between the Fermi and vacuum energy. Analogous phenomena occur in Ni, where they have been studied in detail. (The relation of the present data to the Ni data is discussed in Sec. V.)

To summarize: Reasonable evidence exists to suggest that the low KE structure in the EDC's for $h\nu > 10.2$ eV is due to filled band states and not to the emission of electron-electron scattered electrons. The assumption that the low KE part is due to nondirect transitions is supported by inference only. The resultant density of states obtained by the arguments above is shown in Fig. 8. Some contribution by scattered electrons is expected, but the effect is not analytically investigated in the present study. The analysis presented indicates that the scattering does not dominate.

C. Liquid-Air Temperature Dependence

The absence of significant temperature changes in the yield or energy distribution in the temperature range 85–300°K indicates that the transitions observed do not involve interaction with phonons. The probability of the conventional phonon-dependent indirect transition depends on the phonon density.[1,14] As the phonon population decreases with temperature, the probability of the transition should decrease. This is not observed in these measurements. Even though the yield changes observed on cooling are about of the same magnitude as the expected error, they are consistently positive, which is the opposite of a phonon process. Increased yields for cooled samples are reported by Taft and Philipp.[15]

An increase in the quantum yield can be understood in terms of scattering processes. As previously described,[1] scattering in photoemission can be divided into two classes: phonon scattering, which is essentially elastic because the energy losses (mV) are small, compared with the parameters of the experiment; and electron-electron scattering, which is inelastic. As the temperature increases, the phonon scattering increases the escape path and the probability of electron-electron scattering is increased. This would make the yield at room temperature smaller because most of the inelastically scattered electrons have energies less than the threshold.

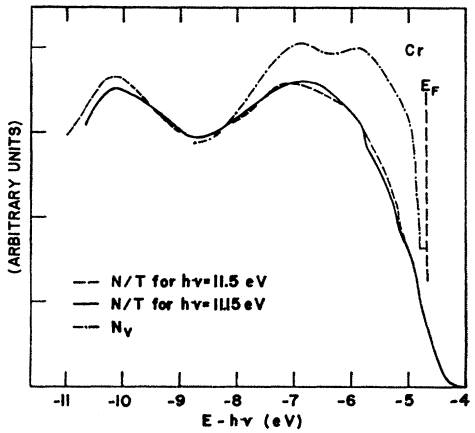

FIG. 11. The energy distributions divided by the escape function for photon energies of 11.15 and 11.5 eV plotted versus $E-h\nu$ and the optical density of states for $-4 \leq E-E_F \leq 0$ eV shifted by the work function.

D. Temperature Dependence above the Néel Point

The negligible changes observed in the yield and EDC's between room temperature and temperatures above the Néel temperature indicate that any shifts in the density of states due to magnetic ordering are too small to be measured by this technique. Since the resolution of the experiment is a few tenths of an eV, energy shifts in the electronic structure are no greater than about 0.3 eV. Absence of measurable effects has been observed in photoemission studies on Gd,[16] ferromagnetic Al–Ni alloys,[17] and preliminary studies on Ni.[2]

E. Yield and RFR at $h\nu = 9.4$ eV

At 9.4 eV, the yield and RFR each has a minimum which showed some sample dependence. This sample dependence was not studied in detail in these experiments. Tentatively the phenomena are interpreted as being due to a surface or impurity plasmon.[18] Electron energy-loss measurements show a characteristic peak in this energy region, which is not attributed to the "classical" plasmon.[19] The energy-loss measurements are sample-dependent.[20] The EDC at this energy show no major changes although a slightly increased attenu-

[14] L. H. Hall, J. Bardeen, and F. J. Blatt, Phys. Rev. **95**, 559 (1954).
[15] E. A. Taft and H. R. Philipp, Phys. Rev. **115**, 158 (1959).
[16] A. J. Blodgett, Jr., W. E. Spicer, and A. Y.-C. Yu, in *Optical Properties and Electronic Structure of Metals and Alloys* (North-Holland Publishing Co., Amsterdam, 1966), pp. 246–256.
[17] W. M. Breen, F. Wooten, and T. Huen, Phys. Rev. **159**, 475 (1967).
[18] E. A. Sziklas, Phys. Rev. **138**, A1070 (1965).
[19] L. Marton and L. B. Leder, Phys. Rev. **94**, 203 (1954).
[20] L. Marton, Rev. Mod. Phys. **28**, 172 (1956).

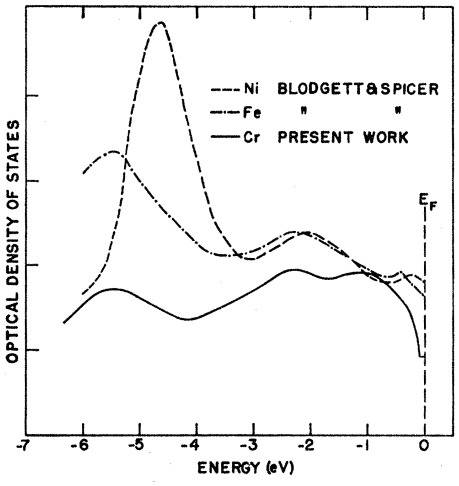

FIG. 12. The filled band optical density of states for nickel, iron, and chromium. The nickel and iron curves are after Blodgett and Spicer (Refs. 2 and 4).

ation is indicated near maximum KE (see Fig. 5). This is to be expected since the photon absorption depth is greater.

V. DISCUSSION OF RESULTS

The photoemission investigation on evaporated films of Cr has been made in the spectral range from 4.68 (threshold) to 11.8 eV at 85, 300, and >323°K. The study shows that the optical excitations are nondirect for the transition between the filled band at $-4 \leq E-E_F \leq 0$ eV to empty band at $4.7 \leq E-E_F \leq 11.8$ eV. The observation is made that: (1) **k** conservation is not an important selection rule, (2) the bands are not so narrow that the **k** values are degenerate, and (3) the transitions are not phonon-assisted as in the indirect transition.

Using the nondirect transition model of Spicer *et al.*, the optical density of states for $-4<E-E_F<0$ and $4.68<E-E_F<11.8$ is obtained. The matrix elements for the excitations are found to be approximately constant. Reasonable evidence is presented for the existance of valence band states around −5.5 eV. These deep states are analyzed with the nondirect model, and the optical density of states is obtained. The experimental limits on the spectral range prohibit direct determination that excitations from the deep states are nondirect. The optical density of states for Cr including the anomalous peak in the neighborhood of −5.5 eV is displayed with the density of states for Fe [4] and Ni [2] in Fig. 12. The optical density of states for Co has been measured but is omitted for simplicity since it is consistent with the results for Fe and Ni. The magnitudes of the curves in Fig. 12 are arbitrary.

The optical density of states for Cr is surprisingly similar to those for Fe, Co, and Ni. The anomalous peak found in Fe, Co, and Ni is tentatively observed in Cr at -5.5 ± 0.3 eV. The magnitude of the anomalous peak in Cr is smaller, as the behavior in the Ni, Co, and Fe sequence would suggest. The peak position in Cr, however, is about the same as the peak position in Fe, whereas the behavior of the position in the sequence Ni, Co, Fe shows a shift to lower energy. Since the peak in Cr appears very near the threshold in the EDC's, its exact position is difficult to determine. Yu and Spicer[3] have suggested that the anomalous peak in Ni, Co, and Fe is associated with ferromagnetism since the peak is not observed in the paramagnetic metals that have been studied. This interpretation is consistent with the present observation since Cr is antiferromagnetic. The width of the structure at energies above the anomalous peak is very nearly the same in the different metals. This similarity shows that the rigid-band model is not valid for extrapolation between Cr and Fe. The Cr density of states is not obtained from the Fe density of states when the Fermi energy is lowered so that the filled states contain two less electrons. This result is not dependent on the interpretation of the anomalous peak.

Cr has two features which are different from Fe and Ni, (see Fig. 11). First, Cr shows two intermediate peaks (1.1 ± 0.2 and 2.2 ± 0.2 eV) below the Fermi energy in addition to a shoulder at −0.2 eV, whereas Fe, Co, and Ni have a broad intermediate peak and a small peak a few tenths eV below the Fermi energy. Second, a low density of states at the Fermi energy is observed.

The low optical density of states at the Fermi energy correlates with the density of states obtained from low-temperature electronic specific-heat measurements. In Fig. 13, the density of states in the region near the Fermi energy is plotted, together with the density of states obtained from specific-heat measurements on alloy sequences (Cr with V).[21] The correlation is made between the small shoulder observed in the photoemission data (see Sec. III A) and the flat region for dilute alloys of Cr with V and not with the specific-heat value for pure Cr. Since the resolution of the present experiments is a few tenths of an eV, the detailed structure at the Fermi energy is not observable. The magnitude of the optical density of states is obtained by extrapolating the results shown in Fig. 8 to zero at −7.0 eV and setting the area equal to 6 electrons per atom. The procedure gives the values of 1.07 and 0.43 electrons per atom per eV at the maximum and Fermi energy, respectively. The specific-heat value near the Fermi energy is about 0.46 electrons per atom per eV. Since the low-energy density of states is obtained from limited data and corrections are not made for electrons scattered into the EDC's, the quantitative correlation is better than might be expected. The use of specific-heat data from alloy sequences to obtain the density of states is dependent on the rigid-band model. Because

[21] C. H. Cheng, C. T. Wei, and P. H. Beck, Phys. Rev. **120**, 426 (1960).

the rigid-band model is invalid for the 3d-transition metals (see the discussion above), the disagreement in Fig. 13 at larger energies is not unexpected.

Attaching significance to the small electron concentration changes in the specific-heat technique is not necessarily inconsistent with not attaching significance to the techniques for finding the density of states deep in the bands which require large electron concentration changes. Limited correlation between the two techniques for energies near the Fermi energy is obtained in the studies on Ni.[2] Photoemission studies on Ni alloyed with Al (which has a relatively simple electronic structure) show that limited changes in electron concentration move the Fermi energy up in the essentially Ni density of states.[20]

Present band calculations for Cr are in major disagreement with the photoemission results, particularly in the case of the deep anomalous peak. The d-band calculations of Osdente and Friedel[22] for Cr show no states in the energy region where the anomalous peak is observed. Similar discrepancies are reported and discussed in the studies on Fe, Co, and Ni.[3] Several explanations for these previously reported anomalous peaks have been suggested. Philips[23] has proposed a many-body resonance model, and Mott[24] in discussing the Ni data suggests that a $4s^23d^8$ configuration may cause the states.

On comparing the calculated density of states[22] with photoemission results for energies between the anomalous peak and the Fermi energy, several features should be pointed out. The calculated filled bandwidth is about 2.2 eV whereas the width of the observed states above the anomalous peak is about 3.5 eV. Although the calculated width is too narrow, two qualitative features of agreement can be pointed out. First, the calculated results show generally three peaks, as the data do for $E-E_F>3.5$ eV. Second, the calculations show a low density of states at the Fermi energy. The details of the above calculated features, however, do not correlate with the present measurements. It is suggested that the band calculations for Cr can be used to obtain results for neighboring metals in the periodic table by application of the rigid-band model. As pointed out above, this is not true for the series Cr, Fe, Co, and Ni.

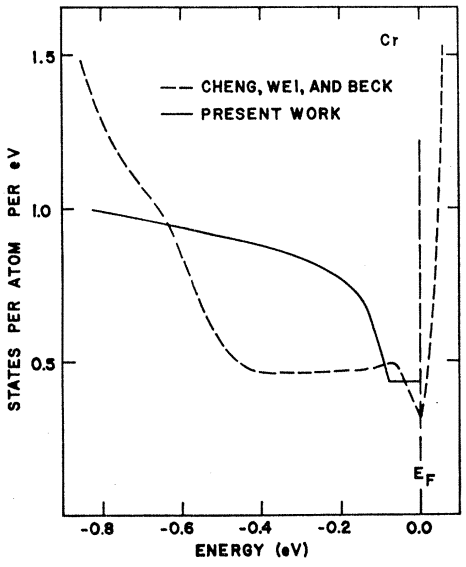

FIG. 13. Comparison near the Fermi energy of the optical density of states for chromium to the density of states obtained from specific measurements after Cheng, Wei, and Beck (Ref. 21).

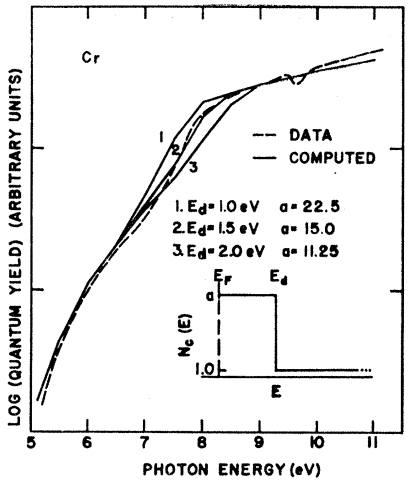

FIG. 14. Comparison of the spectral dependence of the measured quantum yield to computed yields for three different empty d-band states with widths of 1.0, 1.5, and 2.0 eV. The area of each empty d band is the same.

The upper limit of approximately 0.3 eV, which these experiments place on shifts in the density of states when the temperature is increased above the Néel temperature, is consistent with the results obtained for other measurements above and below magnetic ordering temperature. At present, studies have been reported on Gd,[24] ferromagnetic Ni–Al alloy,[20] and Ni. The Ni studies above the Curie temperature are preliminary.[2]

A technique is presented for obtaining reflectance information from a photodiode. The semiquantitative measure of the reflectance (see Fig. 1) has a peak at 6.8 eV and a pronounced shoulder at about 8 eV. The general nature of the reflectance is similar to that observed for Ni[25] and Fe.[4] In the sequence Ni, Fe, and Cr, the structure occurs at successively higher energies and the level of the reflectance decreases.

[22] M. Osdente and J. Friedel, Phys. Rev. **124**, 384 (1961). More recent calculations are made by T. L. Loucks, *ibid.* **139**, A1181 (1965). The results are in general agreement but do not include a density-of-states computation.

[23] J. C. Phillips, Phys. Rev. **140**, A1254 (1965).

[24] N. F. Mott, in *Optical Properties and Electronic Structure of Metals and Alloys* (North-Holland Publishing Co., Amsterdam, 1966), p. 314.

[25] H. Ehrenreich, H. R. Philipp, and D. J. Olechna, Phys. Rev. **131**, 2469 (1963).

The reflectance structure observed in Cr correlates with the anomalous peak observed in the optical density of states, just as the reflectance data and anomalous peak correlate in the studies on Ni [2] and Fe.[4]

ACKNOWLEDGMENTS

We gratefully acknowledge discussions with W. E. Spicer and co-workers throughout the course of this investigation. Discussion with F. Wooten is also acknowledged. We thank R. Evans and F. Blankenberg for construction of the electronics used in this investigation.

APPENDIX

The spectral distribution of the quantum yield is influenced by the optical density of states between the Fermi energy and vacuum energy. The dependence is used to obtain the approximate character of the empty d bands. The presently available optical data and the spectral limits of the photoemission data are too limited for a detailed analysis.

For the case in which the absorption coefficient $\alpha(h\nu)$ is much greater than the reciprocal of the scattering attenuation length, the quantum yield in the nondirect model is given by the following equation[1]:

$$Y(h\nu)=\int_{E_\phi}^{E_F+h\nu} T(E)N_c(E)N_v(E-h\nu)\,dE \Big/ \int_{E_F}^{E_F+h\nu} N_c(E)N_v(E-h\nu)\,dE. \quad (4)$$

The functions are defined in Eq. (2), and the matrix elements are assumed to be independent of E. Inspection of Eq. (4) shows that the character of the spectral dependence of the quantum yield is determined by the competition between optical excitations which produce emission and excitations that do not. Excitations which do not produce emission, the denominator of Eq. (4), are determined by the states between the Fermi energy and vacuum energy.

The strong increase observed in the quantum yield in the neighborhood of 7 eV (see Fig. 2) results when the final states of the excitations are no longer the high-density d-band states but the low-density states above the d band. By trial and error, an approximation for the empty d band was obtained by comparing calculations using Eq. (4) with the data in Fig. 2. For the calculations the functions were represented by 0.5-eV histograms. A square d band was used, and a reasonable fit was obtained for a width of 1.5 eV and a height ratio relative to the constant density of states above the d band of 15/1. The computed results are compared to the yield (electrons per incident photon) in Fig. 14. The curves are arbitrarily normalized at $h\nu=9$ eV. The results for widths of 1.0, 1.5, and 2.0 eV with constant d-band areas are shown. The computations require knowledge of the N_v for $E-E_F<-6$ eV. Since the data are not available, N_v is assumed to go to zero at -7 eV. It is reasonable to assume that s-band states only exist below -7 eV and that they should make a minor contribution to the denominator of Eq. (4). Because a constant multiplier for N_c and N_v cancel in Eq. (4), the calculated results should give numbers with correct magnitudes. The calculated magnitude is too large, which indicates that scattering effects need to be accounted for. To examine this feature and to do a detailed study, the scattering length and optical data are needed but are not presently available.

The approximate results for the empty states are in better agreement with band calculations[22] than the filled band results. The band calculations and the specific-heat results[21] (Fig. 13) indicate that the density of states for the empty d bands increases sharply above the Fermi energy.

Errata

Equations of Motion of Nuclear Magnetism, BALDWIN ROBERTSON [Phys. Rev. **153,** 391 (1967)].

1. In Eq. (23) there should not be a tilde over the K on the right.
2. In Eq. (24) there should be a dt' on the right.
3. In Eq. (34) there should be a minus sign before the λ on the right.
4. In the paragraph containing Eq. (36), the last sentence should read: Because of Eqs. (33), (34), and (35), $\tilde{K}_\lambda{}^{\mu,-\mu}$ is now an even function of t and is real.
5. In the equation in the first line below Eq. (50), there should be a caret over the F on the left.
6. Equation (53) needs an angular bracket.
7. In Eq. (B6) the last term on the right side should not have M in the denominator.
8. Equation (12) should have a bar over the leftmost A.
9. Throughout the paper, the word *dyad* should be replaced by the word *dyadic.*

Statistical Mechanics and Origin of the Magnetoelectric Effect in Cr_2O_3, R. HORNREICH AND S. SHTRIKMAN [Phys. Rev. **161,** 506 (1967)]. The sign before the third term on the right in Eq. (1) should be $\mp$ rather than $\pm$. The values of $|b_\perp'|$ in Table I should be multiplied by 2. We are indebted to Dr. M. Mercier for pointing out these errors.